Available online at www.sciencedirect.com
ScienceDirect
Energy and Buildings 40 (2008) 702–709
ENERGY and BUILDINGS
www.elsevier.com/locate/enbuild

Energetic and exergetic performance investigation of the Bigadic Geothermal District Heating System in Turkey

Z. Oktay [a,b,1], C. Coskun [b], I. Dincer [a,*]

[a] Faculty of Engineering and Applied Science, University of Ontario Institute of Technology (UOIT), 2000 Simcoe St. N., Oshawa, ON L1H 7K4, Canada
[b] Mechanical Engineering Department, Faculty of Engineering, Balikesir University, 10110 Balikesir, Turkey

Received 17 February 2007; received in revised form 5 May 2007; accepted 8 May 2007

Abstract

In this study a comprehensive performance analysis of the Bigadic Geothermal District Heating System (GDHS) in Balikesir, Turkey is performed through thermodynamic assessment in terms of energy and exergy efficiencies. The actual thermal data taken from the Technical Department of the GDHS are utilized in the analysis to determine the exergy destructions in each component of the system and the overall energy and exergy efficiencies of the system for two reference temperatures taken as 15.6 °C for November (e.g., case 1) and 11 °C for December (e.g., case 2). The energy and exergy flow diagrams are clearly drawn to illustrate how much destructions/losses take place in addition to the inputs and outputs. The average energy and exergy efficiencies are found to be 30% and 36% for case 1, and 40% and 49% for case 2, respectively. The key reason as to why the exergy efficiencies are higher is because the heat recovery option is used through the reinjection processes which make use of waste heat. A parametric study is also conducted to show how energy and exergy flows change with the environment temperature. The results are expected to be helpful to researchers and engineers in the area.

Keywords: District heating; Geothermal energy; Performance; Energy; Exergy; Efficiency

1. Introduction

Recently, some potential solutions to the possible problems associated with greenhouse gas emissions have evolved, including: energy conservation through improved energy efficiency, switching from fossil fuels to more environmentally benign energy forms (including increased use of renewable energy sources and technologies), acceleration of forestation to absorb CO_2, and reduced energy usage by changing life styles and increasing public awareness. In this regard, geothermal energy appears to be one of key solutions to both current and future energy and environment solutions.

Geothermal district heating, with Iceland in the forefront, has been one of the fastest growing segments of the geothermal industry and now accounts for over 75% of all space heating based on geothermal fluids [1]. Bloomquist [2] pointed out that ''Turkey is installing new geothermal district heating systems at a fast pace and may soon emerge as a leader in this field''.

During the past two decades there has been increasing interest in using geothermal district heating systems extensively in various countries (France, Iceland, USA, China, Japan, Turkey, etc.). Turkey is one of the top five countries for geothermal direct applications [1] because of its large number of geothermal district heating systems. Table 1 lists the geothermal district heating systems installed in Turkey and their technical details for comparison purposes.

In this study, the Bigadic Geothermal District Heating System (GDHS), the longest geothermal pipeline in Turkey (and world's third longest one), is investigated. In the Bigadic GDHS, the required mass flow rates according to the changing conditions in district heating system are controlled manually. The mass flow rates are not automatically controlled and therefore the data are insufficient. It was observed that there is an uncertainty about the process of controlling the mass flow rate. Due to this reason, to make an

* Corresponding author. Tel.: +1 905 721 8668; fax: +1 905 721 3370.
E-mail addresses: zuhal.oktay@uoit.ca (Z. Oktay), canco82@yahoo.com (C. Coskun), ibrahim.dincer@uoit.ca (I. Dincer).
[1] Currently on her sabbatical at UOIT.

0378-7788/$ – see front matter © 2007 Elsevier B.V. All rights reserved.
doi:10.1016/j.enbuild.2007.05.004

Nomenclature

C_f	specific heat of the fluid (kJ/(kg °C))
$\dot{E}$	energy rate (kW)
$\dot{E}_{design}$	heat requirement for colder or ''winter'' months (kW)
$\dot{E}_{smr}$	heat requirement for hot water during warmer or ''summer'' months (kW)
Ėx	exergy rate (kW)
h	specific enthalpy (kJ/kg)
$\dot{m}$	mass flow rate (kg/s)
N_{dw}	number of (average) dwellings
N_{per}	number of persons per average dwelling
N_{warm}	number of warmer or ''summer'' days
P	pressure (kPa)
s	specific entropy (kJ/(kg K))
S	average daily usage of sanitary hot water [kg/(person-day)]
T	temperature (°C or K)
$\Delta T_{average}$	difference between the indoor and average outdoor temperatures (°C)
ΔT_{design}	difference between the indoor and minimum outdoor temperatures (°C)
T_{indoor}	indoor temperature (°C)
$T_{outdoor}$	outdoor temperature (°C)
T_R	temperature ratio
ΔT_w	difference in water temperatures (°C)

Greek symbols

η	energy or first law efficiency (%)
ε	exergy or exergetic or second law efficiency(%)
ψ	flow exergy (kJ/kg)

Subscripts

d	destroyed
he	heat exchanger
in	inlet
out	outlet
pi	pipe
pu	pump
sys	system
T	total
tw	thermal water

accurate analysis, the required data are collected on two different dates for comparison purposes. Using these different data sets, we aim to find the energy and exergy values and the exergy destructions along with efficiencies during the operation of the system. In recent years there has been an increasing interest in Turkey by various researchers (e.g., [4–9]) to study the geothermal district energy systems through energy and exergy analyses. Furthermore, in order to evaluate the system performance and its variation during operation, a parametric study is conducted with the temperature, pressure and mass flow rate values, varying with various reference temperature values.

2. Case study: Bigadic Geothermal District Heating System

The Bigadic geothermal field is located 38 km south of the city of Balıkesir which is in the west of Turkey. Bigadic geothermal field covers a total used area of about 1 km^2. The reservoir temperature is taken as 110 °C. As of the end of 2006, there were two wells (namely HK-2 with a depth of 429 m and HK-3 with a depth of 307 m, respectively). The well head temperature is 98 °C. Moreover, there are five pumps in the Bigadic geothermal field. Three pumps are used for the wells and the remaining ones are used to pump fluid to the mechanical room. Wells 1 and 2 are basically artesian wells through which water is forced upward under pressure. Pumps 1 and 2 were in use but not pump 3 on the days the data were taken. Pump 3 is designed to pump automatically when the mass flow rate requirements achieve 100 kg/s. During our study, this pump did not work because of the low mass flow rate requirements. The mass flow rate was equal to 53 kg/s and 63.8 kg/s when the temperature and pressure values were used as actual data based on November and December 2006, respectively. Moreover, Pump 3 generally is not used because of the elevation distance between the geothermal source and the mechanical room. This elevation distance is 200 m and provides enough pressure that is needed to convey the fluid. If the mass flow rate demand increases significantly, Pump 3 will work automatically.

Here, we can explain the system in three main parts (Fig. 1). In the first part, the geothermal fluid is pumped into the 'mud and gas separator unit' to separate harmful particles. After passing through the mud and gas separator unit, the geothermal fluid flows to the first heat exchanger. There is an 18 km long pipeline between the geothermal source and the mechanical room. In-between the geothermal source and the mechanical room, the geothermal fluid temperature decreases by about 3–4 °C, respectively.

In the second part, the geothermal fluid is cooled to approximately 44 °C in the first and second heat exchangers constructed in the mechanical room. After the heat transfer taking place in the first and second heat exchangers, the geothermal fluid is sent to the first and second center-pipelines. A second fluid (clean water) enters the first and second heat exchangers with a temperature of 47 °C and leaves measuring 68 °C (on 6 December 2006).

In the third part, clean hot water is pumped to the heat exchangers which were constructed under each building. The system is designed to have one or two heat exchangers for each building. One heat exchanger is for heating, and the other is for hot water requirements. Presently, each building has one or two heat exchangers to supply heat and hot water requirements. Ten percent of the total residence in Bigadic has an extra heat exchanger for hot water requirements. There are three pipelines to convey the hot water along the different paths. The second and third center-pipelines are in use. The first center-pipeline is not in use yet.

The second and third center-pipelines are designed to carry 15,253 kW of heat to the 2200 individual residences. The indoor and outdoor design temperatures equal 20 °C and

Table 1
Geothermal district heating systems installed in Turkey

Location	Province	Capacity (MW_t)	Geothermal fluid temperatures (°C)	Year commissioned	Network supply/return temperatures (°C)[a]	Installed capacity/number of dwellings heated
Gonen	Balikesir	32	80	June 1987	–	4500/3400
Simav	Kutahya	25	120	October 1991	65/50	6500/3200
Kirsehir	Kirsehir	18	54–57	March 1994	48/42	1800/1800
Kizilcahama	Ankara	25	80	November 1995	–	2500/2500
Balcova	Izmir	72	115	October 1996	85/60	20,000/6849
Kozakli	Nevsehir	11.2	90	1996	–	1250/1000
Afyon	Afyon	40	95	October 1996	60/45	10,000/4000
Sandikli	Afyon	45	70	March 1998	70/40	5000/1700
Diyadin[b]	Agri	42	78	–	78/45	2000/1037
Salihli	Manisa	142	94	September 1998	–	2400/20,000
Bigadic	Balikesir	31.83	98	November 2004	78/43	2200/3000
Edremit	Balikesir	10.33	60	2003	58/38	1650/7500

[a] Average values are given.
[b] An integrated geothermal application system consisting of district heating, agriculture (greenhouse heating), bathing and balneology (thermal hotel), aquaculture (fishing pond), industrial processes (liquefied carbon dioxide and precipitated calcium carbonate productions). Source: [3,4].

−6 °C, respectively. The second and third center-pipelines supply the heat requirement of the dwellings, one post office, one dormitory, eight colleges, one state hospital, two police stations and ten government agency buildings.

Throughout the study, the heat exchangers for all the residences were thought to act like one heat exchanger. All the heat from the heat exchangers on the second center-pipeline is collected to one heat exchanger called 'Heat Exchanger 3'. In the same method, all the heat from the heat exchangers on the third center-pipeline is collected to one heat exchanger called 'Heat Exchanger 4'. The heat is then transferred to the highest and longest points. The state hospital has both the highest elevation distance and the longest pipeline distance when considering the mechanical room. The state hospital is determined as a critical point for calculations. The temperature and pressure values were taken from the state hospital.

The same mark plate-type heat exchangers are used in the system. Inlet and outlet heat exchanger liquid temperatures were investigated from the state hospital.

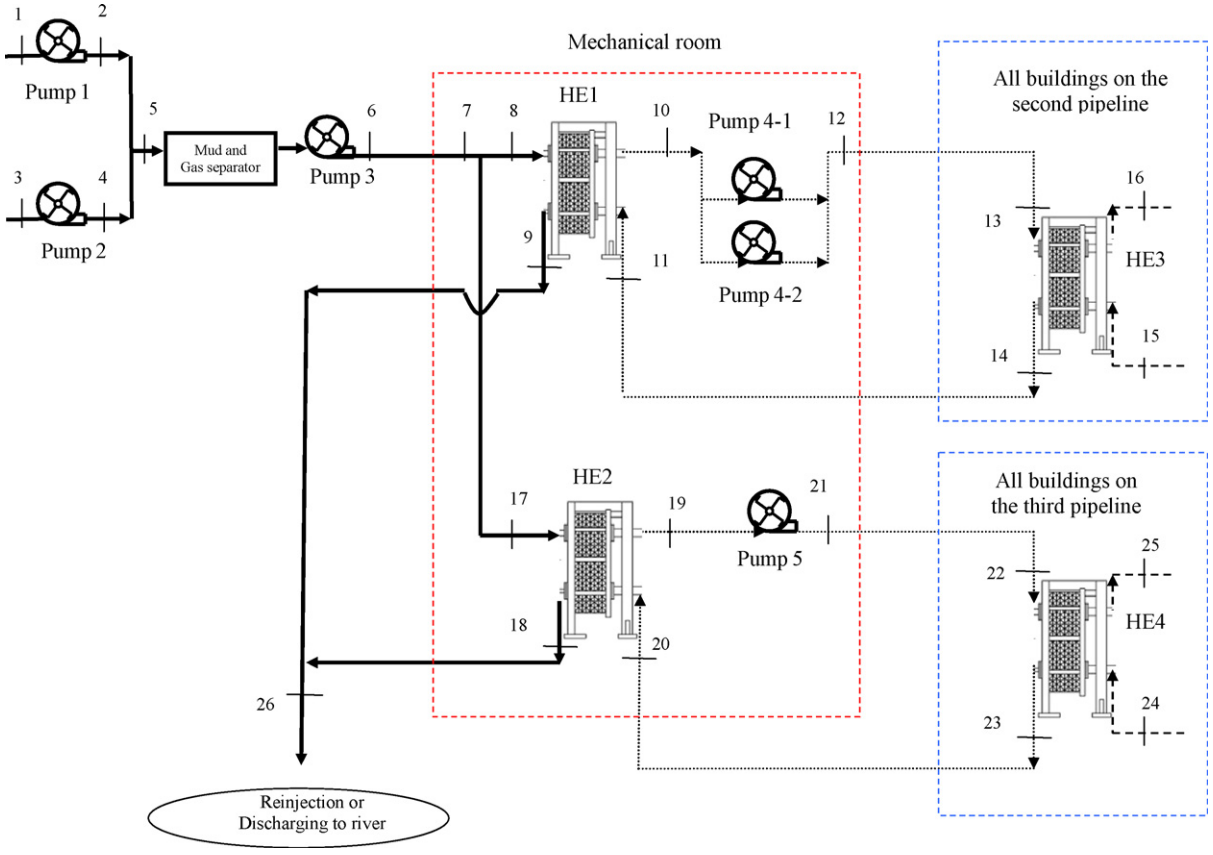

Fig. 1. Flow chart of the Bigadic GDHS.

3. Analysis

3.1. Balance equations

Here the balance equations are written for mass, energy and exergy flows for the system and its components, by considering the steady-state and steady-flow process in engineering thermodynamics. These are basically the general equations as also used by some earlier researchers (e.g., [5–10]).

The mass balance equation for the overall geothermal system can be written as:

$$\dot{m}_{T,in} = \dot{m}_{T,out} \tag{1}$$

where $\dot{m}_T$ is the total mass flow rate (kg/s).

The geothermal water energy and exergy values are calculated from the following equations:

$$\dot{E}_{T,in} = \dot{m}_{tw} h_{tw} \cong \dot{m}_{tw,2} h_2 + \dot{m}_{tw,3} h_3 \tag{2}$$

$$\dot{E}x_{T,in} = \dot{m}_{tw,2}[(h_{tw,2} - h_0) - T_0(s_{tw,2} - s_0)] + \dot{m}_{tw,3} \lfloor (h_{tw,3} - h_0) - T_0(s_{tw,3} - s_0) \rfloor \tag{3}$$

where the subscripts 2 and 3 denote the working wells.

The exergy destructions in the heat exchanger, pump and system itself are calculated by using these equations:

$$\dot{E}x_{d,he} = \dot{E}x_{in} - \dot{E}x_{out} \quad \text{for heat exchanger} \tag{4}$$

$$\dot{E}x_{d,pu} = \dot{W}_{pu} - (\dot{E}x_{out} - \dot{E}x_{in}) \quad \text{for pumps} \tag{5}$$

$$\dot{E}x_{d,pi} = \dot{E}x_{in} - \dot{E}x_{out} - \dot{E}x^{Q} \quad \text{for pipes/pipelines} \tag{6}$$

$$\dot{E}x_{T,d} = \dot{E}x_{T,d,he} + \dot{E}x_{T,d,pu} + \dot{E}x_{T,d,pi} \tag{7}$$

The energy efficiency of the system is determined using the following equation:

$$\eta_{sys} = \frac{\dot{E}_{T,out}}{\dot{E}_{T,in}} \tag{8}$$

where $\dot{E}_{T,out}$ is the total exergy output (useful heat) and $\dot{E}_{T,in}$ is the total exergy input.

The exergy efficiency of a heat exchanger is basically defined as the ratio of the exergy output (i.e., increase in the exergy rate of the cold stream) to the exergy input (i.e., decrease in the exergy rate of the hot stream) as follows:

$$\varepsilon_{he} = \frac{\dot{m}_{cold}(\psi_{cold,out} - \psi_{cold,in})}{\dot{m}_{hot}(\psi_{hot,in} - \psi_{hot,out})} \tag{9}$$

The specific exergy (ψ) is represented below:

$$\psi = (h - h_0) - T_0(s - s_0) \tag{10}$$

The exergy efficiency of the system is determined from the following equation:

$$\varepsilon_{sys} = \frac{\dot{E}x_{T,out}}{\dot{E}x_{T,in}} = 1 - \frac{\dot{E}x_{d,sys} + \dot{E}x_{nd}}{\dot{E}x_{T,in}} \tag{11}$$

3.2. Average total residential heat demand

In the "summer" or warmer season (when there is no need to heat the dwellings), during an average of 165 days (i.e., 365−200), only sanitary hot water is supplied to the residences. The total sanitary hot water load over the summer season (Q_s) is given by:

$$\dot{E}_{smr} = N_{dw} N_{warm} N_{per} S \Delta T_w C_f \tag{12}$$

where N_{warm} is the number of warmer days per year as 165, N_{per} the average number of people in each dwelling as 4, S the average daily usage of sanitary hot water as 50 L/(person-day) or 50 kg/(person-day), and ΔT_w is the difference in temperature between that of the sanitary hot water as 60 °C and that of the tab water from the city distribution network as 10 °C. Thus:

$$\dot{E}_{smr} = (2200 \cdot 4 \cdot 50)\text{kg} \cdot (50\,^{\circ}\text{C}) \cdot (4.18\,\text{kJ/kg}\,^{\circ}\text{C}) = 1064\,\text{kW}$$

Here, total "winter" heat demand [sanitary hot water + heating proper] is expressed as:

$$\dot{E}_{design} = \dot{E}_{dw} N_{dw} \tag{13}$$

where N_{dw} is the number of average dwellings and $\dot{E}_{dw}$ is the heat load for an average (or equivalent) dwelling. Taking 2200 residences with a maximum load of 6.9 kW per residence, the overall winter heat load will be 15.25 MW.

Eq. (13) can also be written as:

$$\dot{E}_{design} = \dot{m} C_f \Delta T_{design} N_{dw} \tag{14}$$

where $\Delta T_{design} = (T_{indoor} - T_{outdoor})_{design}$ is the difference between the indoor and outdoor temperatures and becomes $[20 - (-6)]$.

Since the outdoor temperature changes, we need to take in into consideration through $\Delta T_{average} = (T_{indoor} - T_{outdoor})_{average}$ using average outdoor temperatures while the indoor temperature is kept constant. We can now introduce the temperature

Table 2
Bigadic GDHS energy requirements for each month

Months	Average outdoor temperature (°C)	Temperature ratio (T_R)	Total average energy (kW)
For winter months (from Eq. (16))			
October	15.1	0.188	2874.60
November	9.7	0.396	6042.53
December	6.7	0.512	7802.50
January	4.7	0.588	8975.80
February	5.4	0.562	8565.15
March	8.2	0.454	6922.52
April	13.4	0.254	3871.92
For summer months (from Eq. (12))			
May	17.7	–	1064
June	22.4	–	1064
July	24.5	–	1064
August	23.6	–	1064
September	19.9	–	1064

ratio as:

$$T_{\mathrm{R}} = \frac{\Delta T_{\mathrm{average}}}{\Delta T_{\mathrm{design}}} \tag{15}$$

in order to determine the average heat loads, as required, below:

$$\dot{E}_{\mathrm{average}} = T_{\mathrm{R}} E_{\mathrm{design}} \tag{16}$$

Thus, the mass flow rate can be extracted from above equation is:

$$\dot{m} = \frac{\dot{E}_{\mathrm{average}}}{C_{\mathrm{f}}\,\Delta T} \tag{17}$$

Here, Table 2 shows the monthly heat demand breakdown for the each month according to the average outdoor temperatures.

4. Results and discussion

Note that in this study any effects of salts and other components in the geothermal fluid are neglected in getting the thermodynamic properties. The thermodynamic properties of the geothermal fluid were taken like water. Kanoglu [10] also employed this type of selection in the exergy analysis of geothermal power plants. Using general thermodynamic tables and software programs, thermodynamic properties of the water are found (Table 3).

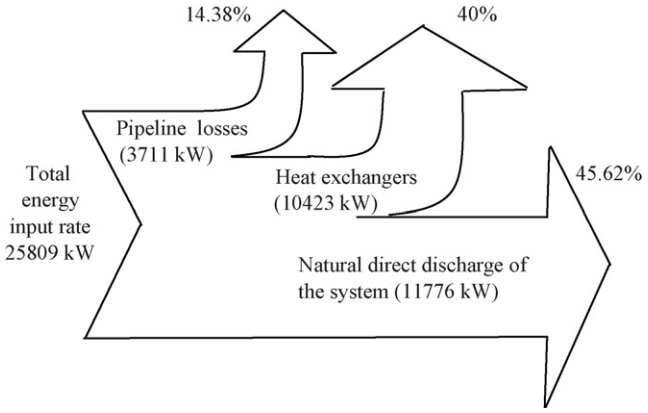

Fig. 2. Energy flow diagram of the Bigadic GDHS for December 2006.

A comprehensive parametric study is presented through the use of actual data that were recorded in November and December 2006. Energy and exergy efficiencies and exergy destructions of the Bigadic GDHS were investigated using these two actual data sets. For each state of the geothermal fluid and hot water, the temperature, pressure, mass flow rate data, energy and exergy rates were calculated using the Engineering Equation Solver (EES) program. In Table 2 an example solution is given based on actual data for December 2006. The state zero shows dead state for both the geothermal fluid and hot water. The dead state conditions are taken as 11 °C and 101.32 kPa for the day considered.

Table 3
Properties of the system fluids, energy and exergy rates at various locations in Bigadic district heating system, Turkey

State no.	Fluid type	Temperature, T (°C)	Pressure, P (kPa)	Specific enthalpy, h (kJ/kg)	Specific entropy, s (kJ/(kg K))	Mass flow rate, $\dot{m}$ (kg/s)	Specific exergy, ψ (kJ/kg)	Exergy rate, $\dot{E}$x (kW)	Energy rate, $\dot{E}$ (kW)
0	TW	11	101.32	46.29	0.166	–	–	–	–
1	TW	97	101.32	406.4	1.273	35	45.66	1598.28	14224.00
2	TW	97.05	404	406.8	1.274	35	45.78	1602.34	14238.00
3	TW	96	101.32	402.2	1.261	28.8	44.87	1292.35	11583.36
4	TW	96.05	404	402.6	1.262	28.8	44.99	1295.69	11594.88
5	TW	96.64	390	405.1	1.268	63.8	45.79	2921.10	25845.38
6	TW	94.5	380	396.1	1.244	63.8	43.60	2781.76	25271.18
7	TW	90	505	377.2	1.192	63.8	39.47	2518.13	24065.36
8	TW	90	505	377.2	1.192	27.15	39.47	1071.59	10240.98
9	TW	47	450	197.2	0.665	27.15	9.25	251.16	5353.98
10	Water	68	152	284.7	0.930	55.55	21.29	1182.77	15815.09
11	Water	47	203	196.9	0.665	55.55	8.92	495.64	10937.80
12	Water	68.06	600	285.3	0.931	55.55	21.78	1209.79	15848.42
13	Water	67.1	253	281	0.919	55.55	20.74	1152.35	15609.55
14	Water	48	152	201.1	0.678	55.55	9.43	523.86	11171.11
15	Water	50	203	209.5	0.704	106.2	10.47	1112.42	22248.90
16	Water	60	182	251.2	0.831	106.2	15.99	1698.48	26677.44
17	TW	90	505	377.2	1.192	36.65	39.47	1446.55	13824.38
18	TW	47	450	197.2	0.665	36.65	9.25	339.04	7227.38
19	Water	68	152	284.7	0.930	75	21.29	1596.90	21352.50
20	Water	47	203	196.9	0.665	75	8.92	669.18	14767.50
21	Water	68.06	600	285.3	0.931	75	21.79	1633.38	21397.50
22	Water	67.1	253	281	0.919	75	20.74	1555.83	21075.00
23	Water	48	152	201.1	0.678	75	9.43	707.28	15082.50
24	Water	50	203	209.5	0.704	143.4	10.47	1502.09	30042.30
25	Water	60	182	251.2	0.831	143.4	15.99	2293.42	36022.08
26	TW	44	400	184.4	0.625	63.8	7.58	483.83	11764.72

Note: state numbers are shown in Fig. 1. Point zero shows reference state (TW: thermal water).

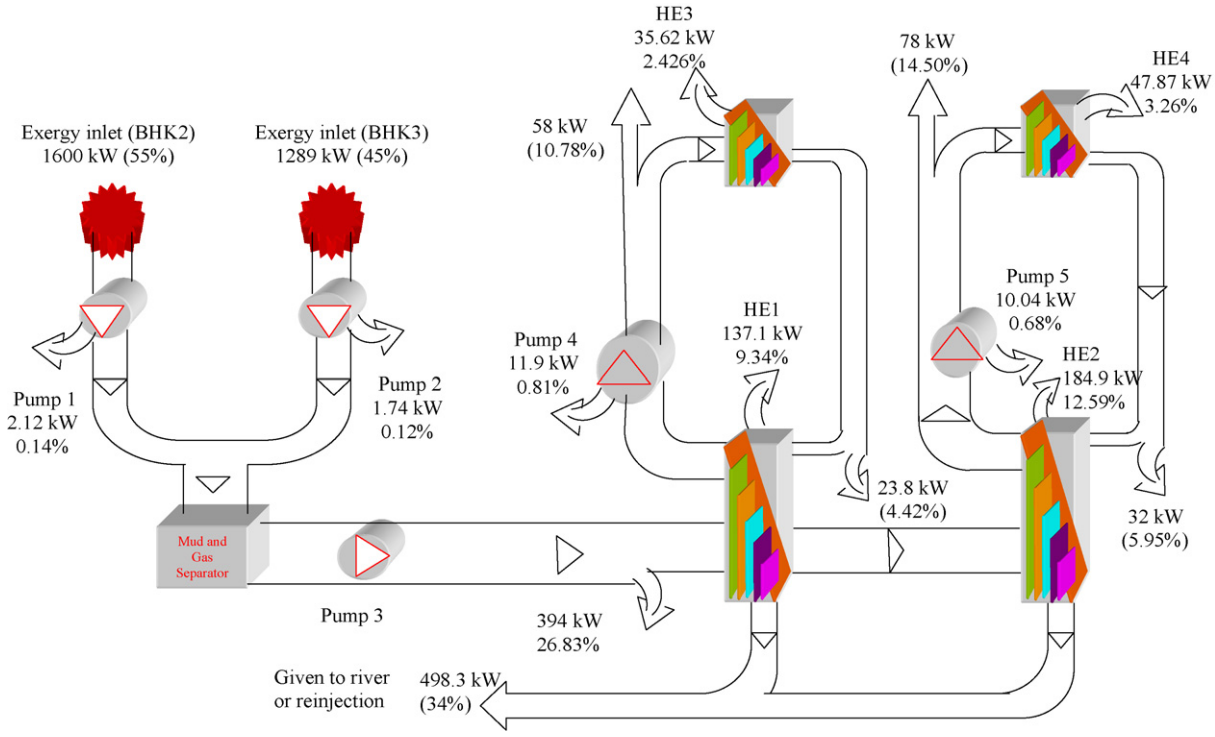

Fig. 3. Exergy inlet of the system, exergy destruction percentage and value of the each part in the system (HE: heat exchanger; BHK: name of the well).

The energy balance diagram is illustrated in Fig. 2. The thermal natural direct discharge accounts for 45.62% of the total energy input, while the pumps and pipeline losses account for 14.38% of the total energy input.

In addition, a detailed exergy flow diagram given in Fig. 3 shows that 51% (corresponding to about 1468 kW) of the total exergy entering the system is lost, while the remaining 49% is utilized. The highest exergy loss (accounting for 37%) occurs from the pipes of the system. The second largest exergy destruction occurs from the thermal natural direct discharge with 34% (corresponding to about 498.3 kW) of the total exergy input. This is followed by the total exergy destruction associated with the heat exchangers and pumps amounting to 405.5 kW and 25.81 kW, which accounts for 26.3% and 1.7% of the total exergy input to the system, respectively.

The energy and exergy efficiencies values were found to be 30% and 36% in November and 40% and 49% in December, respectively. The reference temperatures were 15.6 °C in November and 11 °C in December. Some may see that having higher exergy efficiency may not be accurate. In geothermal systems this is in fact common due to the fact that there is a reinjection process which will allow us to recovery some heat which makes the process/system more exergetically efficient. With the aid of Fig. 4, this situation can be expressed in the following manner: although the input energy value in the system is higher than the input exergy value, the energy losses in the system are higher than the exergy losses. The percentage of the energy losses for November and December were calculated as 70% and 60%, respectively. The exergy destruction percentage for November and December were calculated as 64% and 51%, respectively. Consequently, the exergy efficiency was calculated to be higher because of the fact that the exergy destruction percentage, according to the input exergy value, is less.

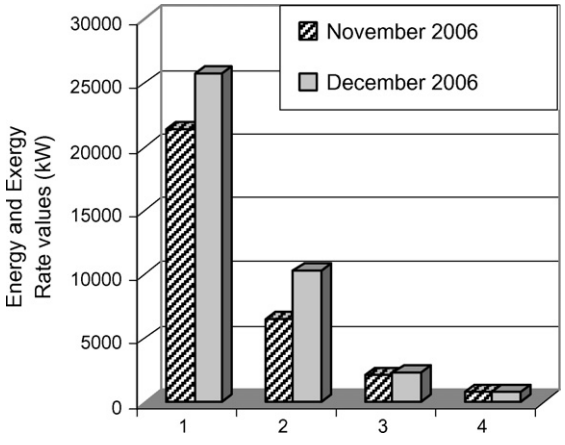

Fig. 4. Energy and exergy values for experimentally studied days (1: $\dot{E}_{in}$; 2: $\dot{E}_{out}$; 3: $\dot{E}x_{in}$; 4: $\dot{E}x_{out}$).

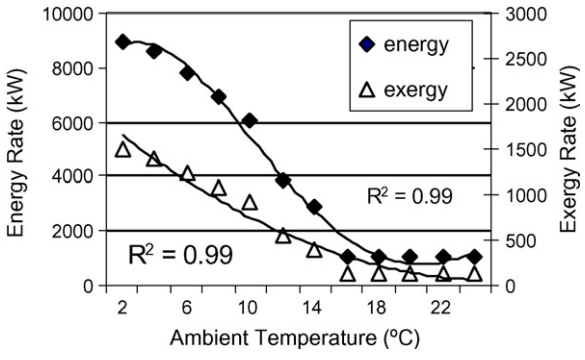

Fig. 5. The profiles of energy and exergy rates as correlated.

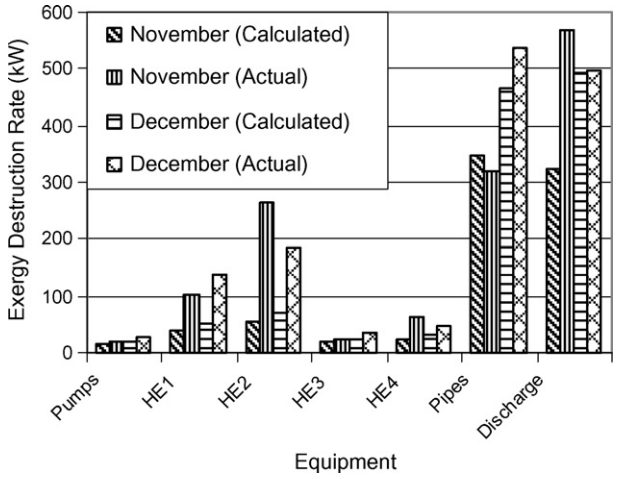

Fig. 6. Comparison of the exergy destructions for various components of the system.

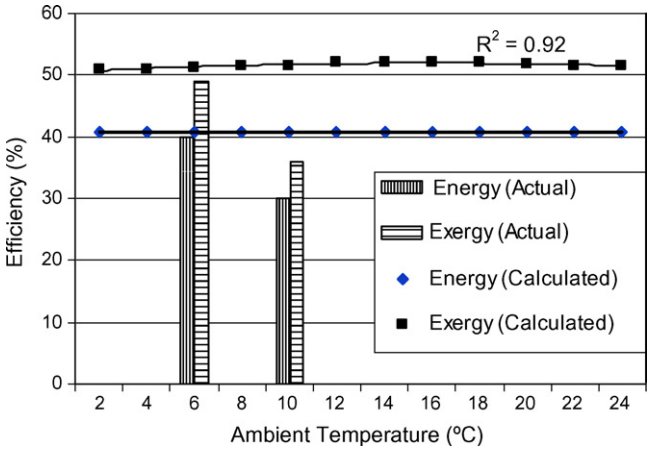

Fig. 8. Energy and exergy efficiency values with ambient temperature (Note: mass flow rates are controlled).

The value of energy demand remains constant during the summer months because during the summer months the hot water is used only for sanitary utilities (see Section 3.2). The energy demand values vary during the winter months depending on outlet temperature. In Fig. 5, the energy demand rates, shown in Table 1, are demonstrated depending on the monthly average outlet (reference) temperature.

Here, energy and exergy demands are aimed to be defined as a function of the reference temperature (e.g., surrounding temperature). This graph was drawn using average values, when the energy and exergy demand values were changing depending on the outlet temperature. Using this figure, a curve fitting is done to predict the demand values for the varying outlet temperatures and the following correlations are obtained:

$$\dot{E} = -1.8543T^4 + 67.761T^3 - 739.89T^2 + 1787.9T + 7679.9 \quad (18)$$

$$\dot{\mathrm{E}}\mathrm{x} = -12.857T^2 - 85.102T + 1609.8 \quad (19)$$

where T is the surrounding temperature taken as the reference temperature (°C). Note that the surrounding temperature must be absolute temperature (in K) in exergy calculations. The aim of developing the correlations with temperatures in celsius is to make easier use for practical applications.

The system was designed to supply the heat loads required for the residences at a constant temperature with variable mass flow rates. Fig. 6 shows both experimental (actual) and calculated exergy destruction magnitudes within the system components, namely pumps, heat exchangers, pipelines and discharge lines, for both months (November and December). As clearly seen, we can make two observations: (i) both actual and calculated irreversibilities show a quite reasonable agreement, except particularly for heat exchangers one and two, and pipelines and (ii) highest exergy destructions (irreversibilities) take place in pipelines and discharge lines where there is a large room for improvement.

Fig. 7 exhibits comprehensive results of monthly exergy destructions as well as inlet and outlet exergies for various components. This helps identify seasonal performance of each system component. One key point from the operational strategies point of view is that the system and hence component efficiency can be made higher through proper control and adjustment of flow rates. Here we go one step ahead to develop the linkage between the exergy efficiency and average air temperature through the following correlation (Fig. 8) as obtained by the curve fitting:

$$\varepsilon_c = -0.0256T^2 + 0.4038T + 50.372$$

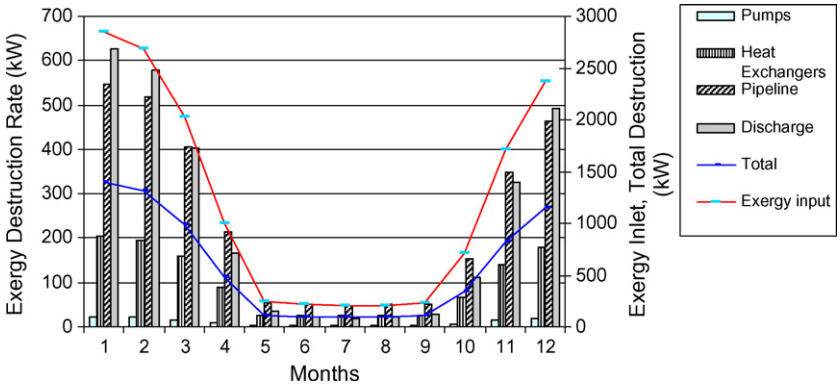

Fig. 7. Monthly exergy inlet and destruction rate values.

In Fig. 8, the two cases are the ones for two days in November and December as the actual.

The Bigadic GDHS does not have a reinjection section yet. This is why the geothermal water flows from the mechanical room to the river at a temperature of about 45 °C. The exergy value of the geothermal water flowing into the river is 498 kW. The exergy efficiency of the system can be increased by the addition of heat pumps and through the use of the geothermal water that is flowing into the river.

5. Conclusions

This paper undertakes a comprehensive performance analysis of the Bigadic geothermal district heating system (GDHS) in Balikesir, Turkey through a thermodynamic assessment in terms of energy and exergy efficiencies. Here are some specific concluding remarks:

- The actual thermal data taken from the Technical Department of the GDHS are utilized in the analysis to determine the exergy destructions in each component of the system, and the overall energy and exergy efficiencies of the system for two reference temperatures taken as 15.6 °C for November (e.g., case 1) and 11 °C for December (e.g., case 2).
- The energy and exergy flow diagrams are clearly drawn to illustrate how much destructions/losses take place in addition to the inputs and outputs. The average energy and exergy efficiencies are found to be 30% and 36% for case 1, and 40% and 49% for case 2, respectively. The key reason as to why the exergy efficiencies are higher is because the heat recovery option is used through the reinjection processes which make use of waste heat.
- Through a parametric study conducted to show how energy and exergy flows change with the environment temperature it is observed that the increase in the system exergy efficiency is due to the increase of the exergy input potential (depending on the decrease of the reference temperature).

The geothermal district heating systems appear to be a potential environmentally benign option that will contribute to the country's economy indirectly because of more economical and efficient heating of the residences. Moreover, this system will help decrease the emission rates.

Acknowledgements

The authors gratefully acknowledge the support of the Balikesir-Bigadic Geothermal Inc. (BBGI) and the personal support of its General Manager, Mr. Ahmet Gurol Yildiz.

References

[1] J.W. Lund, D.H. Freeston, T.L. Boyd, Direct application of geothermal energy, Geothermics 34 (2005) 691–727.
[2] R.G. Bloomquist, Geothermal space heating, Geothermics 32 (2003) 513–526.
[3] BGEI (Bigadic Geothermal Energy Inc.), Reports of Bigadic Geothermal Energy Inc., Unpublished survey/report, Bigadic, Turkey, 2007 (in Turkish).
[4] A. Hepbasli, C. Canakci, Geothermal district heating applications in Turkey: a case study of Izmir-Balcova I, Energy Conversion and Management 44 (2003) 1285–1301.
[5] L. Ozgener, A. Hepbasli, I. Dincer, Thermodynamic analysis of a geothermal district heating system, International Journal of Exergy 2 (3) (2005) 231–245.
[6] Z. Oktay, A. Aslan, Geothermal district heating in Turkey: the gonen case study, Geothermics 36 (2007) 167–182.
[7] L. Ozgener, A. Hepbasli, I. Dincer, Energy and exergy analysis of Salihli geothermal district heating system in Manisa, Turkey International Journal of Energy Research 29 (2005) 393–408.
[8] L. Ozgener, A. Hepbasli, I. Dincer, Performance investigation of two geothermal district heating systems for building applications: energy analysis, Energy and Buildings 38 (2005) 286–292.
[9] L. Ozgener, A. Hepbasli, I. Dincer, M.A. Rosen, Exergoeconomic modeling of geothermal district heating systems for building applications, in: Proceedings of the Ninth International Conference on building simulation, Montreal, Canada, 15–18 August, (2005), pp. 907–914.
[10] M. Kanoglu, Exergy analysis of a dual-level binary geothermal power plant, Geothermics 31 (2002) 709–724.